Molecular dynamics analysis of the effect of electronic polarization on the structure and single-particle dynamics of mixtures of ionic liquids and lithium salts

Volker Lesch, Hadrián Montes-Campos, Trinidad Méndez-Morales, Luis Javier Gallego, Andreas Heuer, Christian Schröder, and Luis M. Varela

Citation: The Journal of Chemical Physics **145**, 204507 (2016); doi: 10.1063/1.4968393
View online: https://doi.org/10.1063/1.4968393
View Table of Contents: http://aip.scitation.org/toc/jcp/145/20
Published by the American Institute of Physics

Molecular dynamics analysis of the effect of electronic polarization on the structure and single-particle dynamics of mixtures of ionic liquids and lithium salts

Volker Lesch,[1,2,a),b)] Hadrián Montes-Campos,[3,a)] Trinidad Méndez-Morales,[3] Luis Javier Gallego,[3] Andreas Heuer,[2,4] Christian Schröder,[5] and Luis M. Varela[3,b)]
[1]*Helmholtz-Institute Münster (IEK-12): Ionics in Energy Storage, Forschungszentrum Jülich, Corrensstrasse 46, 48149 Münster, Germany*
[2]*Institute of Physical Chemistry, Westfälische Wilhelms-Universität Münster, Corrensstrasse 28/30, 48149 Münster, Germany*
[3]*Grupo de Nanomateriais e Materia Branda, Departamento de Física da Materia Condensada, Universidade de Santiago de Compostela, Campus Vida s/n, E-15782 Santiago de Compostela, Spain*
[4]*Center for Multiscale Theory and Computation, Corrensstrasse 40, 48149 Münster, Germany*
[5]*Department of Computational Biological Chemistry, University of Vienna, Währingerstrasse 17, A-1090 Vienna, Austria*

(Received 20 June 2016; accepted 9 November 2016; published online 30 November 2016)

We report a molecular dynamics study on the effect of electronic polarization on the structure and single-particle dynamics of mixtures of the aprotic ionic liquid 1-ethyl-3-methylimidazolium bis-(trifluoromethylsulfonyl)-imide ([EMIM][TFSI]) doped with a lithium salt with the same anion at 298 K and 1 bar. In particular, we analyze the effect of electron density fluctuations on radial distribution functions, velocity autocorrelation functions, cage correlation functions, mean-squared displacements, and vibrational densities of states, comparing the predictions of the quantum-chemistry-based Atomistic Polarizable Potential for Liquids, Electrolytes, & Polymers (APPLE&P) with those of its nonpolarizable version and those of the standard non-polarizable Optimized Potentials for Liquid Simulations-All Atom (OPLS-AA). We found that the structure of the mixture is scarcely modified by the fluctuations in electron charge of their constituents, but their transport properties are indeed quite drastically changed, with larger mobilities being predicted for the different species in the bulk mixtures with the polarizable force field. Specifically, the mean-squared displacements are larger for the polarizable potentials at identical time intervals and the intermediate subdiffusive plateaus are greatly reduced, so the transition to the diffusive regime takes place much earlier than in the non-polarizable media. Moreover, the correlations of the added cations inside their cages are weakened out earlier and their vibrational densities of states are slightly red-shifted, reflecting the weakening effect of the electronic polarization on the Coulomb coupling in these dense ionic media. The comparison of OPLS-AA with non-polarizable APPLE&P indicates that adding polarization to OPLS-AA is not sufficient to achieve results close to experiments. *Published by AIP Publishing.* [http://dx.doi.org/10.1063/1.4968393]

I. INTRODUCTION

Ionic liquids (ILs) are amphiphilic, nanostructured "designer" solvents which form the most promising and abundant category of solvents for several industrial applications due to their now well-known catalog of interesting bulk and interfacial properties,[1–4] including wide electrochemical windows that could make them the next generation of electrolytes in high-tech electrochemical devices such as batteries, supercapacitors, or fuel cells. A precise knowledge of the mechanisms of ion solvation and transport in these dense ionic solvents is essential and many efforts have been devoted to this matter in the past two decades.

The structural and dynamical properties of these systems and their mixtures with cosolvents and electrochemically relevant salts have been extensively studied, both experimentally[5–8] and computationally.[9–13] Computer simulations are powerful tools for the analysis of the microscopic properties of these systems, but an accurate representation of the interparticle interactions must be made in order to achieve acceptable results. It has been reported that the structural properties of these systems are well predicted by simulations with non-polarizable force fields (FFs),[14–16] but neglecting the electronic polarization leads to qualitatively correct but quantitatively unacceptable transport properties of mixtures (see Ref. 10 and references therein). The accuracy of the predictions of structural properties of the non-polarizable potentials has been confirmed by direct comparison of the corresponding results for radial distribution functions (RDFs) of mixtures of ILs and lithium

[a)]V. Lesch and H. Montes-Campos contributed equally to this work.
[b)]Authors to whom correspondence should be addressed. Electronic addresses: luismiguel.varela@usc.es and volkerlesch@uni-muenster.de

salts with X-ray measurements,[17] and the agreement was excellent.

The effect of polarization on structural and dynamical properties of ILs and their mixtures has been reported by Bedrov *et al.*[18] and Lesch *et al.*,[11,13] among others.[9,14,19–25] The pioneering study of the effect of electronic polarization of Yan *et al.*[19] focused on the ionic liquid 1-ethyl-3-methylimidazolium nitrate. They found a strong influence on dynamical properties while structural properties were hardly affected. Bedrov *et al.*[18] reported systematic investigations of the influence of electronic polarization on the accuracy of structural, thermodynamic, and dynamic properties predicted by molecular dynamics (MD) simulations of pure ILs. The authors used the quantum-chemistry-based Atomistic Polarizable Potential for Liquids, Electrolytes, and Polymers (APPLE&P) in its full form and with the atom-based polarizabilities set to zero (APPLE&P-NP) and provided mechanistic understanding of how the influence of polarization in IL simulations leads to stronger correlations in ion-ion distribution functions, which results in a 20%-30% increase in the enthalpy of vaporization and a factor of 2-4 slowing down in translational dynamics as compared to results derived from simulations using the polarizable FFs. These results are contrary to those observed in non-ionic media,[18] suggesting that the electronic polarization essentially influences the Coulomb part of the interatomic potentials.[26]

On the other hand, Lesch *et al.*[11] reported experimental results and simulations of the transport properties of ILs doped with lithium salts, calculating the total ionic conductivity and the ion self-diffusion coefficients. They proved that the agreement between the experimental transport properties and their polarizable simulations was excellent, therefore reaffirming the role of polarization in the transport and dynamic properties of these systems. Moreover, they stated that many-body polarizable terms must be used in the intermolecular potential due to the strong polarization of anions induced by a small lithium cation. This effect of polarization of the IL anions on the environment of Li^+ cations has been also pointed out in several other works.[20,23] Furthermore, the influence of the TFSI oxygen polarizability on the lithium ion transport was recently studied.[13]

However, despite the number of works previously reported on the effect of polarization on the structural and dynamic properties of ILs and their mixtures, we still lack any estimation of the actual effect of polarization in the structure and dynamics of cations of added salts in mixtures with ILs, let alone mixtures with Li salts. From a computational point of view, this can be done by means of a systematic comparison of the structural and dynamic predictions of a commonly used and purely non-polarizable potential like Jorgensen's[27] Optimized Potentials for Liquid Simulations-All Atom (OPLS-AA) and those of APPLE&P. With this comparison, we can grant the preservation of the structure of the mixtures, since OPLS-AA has been previously compared to experimental X-ray measurements.[28] On the other hand, an additional comparison of APPLE&P with its nonpolarizable version would allow to estimate if it is sufficient to add the electronic polarization to conventional OPLS-AA to achieve realistic dynamical results and the actual extent of the influence of electron

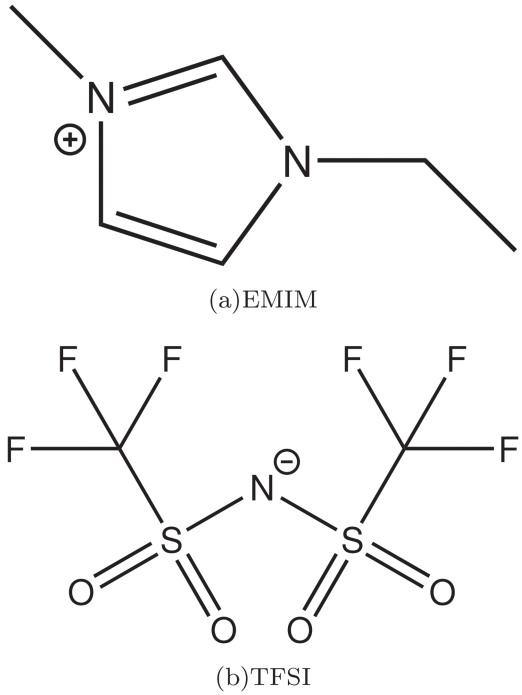

FIG. 1. Molecular structure of 1-ethyl-3-methylimidazolium (a) and bis-(trifluoromethylsulfonyl)-imide (b).

fluctuations in the structure and dynamics of the mixtures. Specifically, despite the importance of this magnitude for ionic transport, the predictions of the cage autocorrelation functions of the added salt cations and their vibrational densities of states depending on the used potential—and, hence, the influence of polarizability—have not been compared up to now.

These are the main aims of the current work, in which we performed the first direct comparison for mixtures of these dense ionic solvents and lithium salts that share the anion using two optimized potentials and the non-polarizable version of APPLE&P to estimate the order of magnitude of the influence of electronic polarization. More specifically, we simulated mixtures of 1-ethyl-3-methylimidazolium bis -(trifluoromethylsulfonyl)-imide ([EMIM][TSFI]; see Fig. 1) and Li[TFSI], and we focused on the description of both the structures of the mixtures and the single-particle dynamics of Li^+ cations in the bulk with all these force fields, and systematically compared their predictions.

The remainder of this paper is organized as follows: In Sec. II, we provide a detailed description of the induced point dipole method, followed by the computational procedures employed in this study; next, we present and discuss the obtained results, and in Sec. V we summarize our main conclusions.

II. THEORETICAL SECTION

A detailed description of the actual influence of electronic fluctuations on the condensed phase behavior of ionic media demands the evaluation of the effect of these degrees of freedom in the intermolecular interaction potentials. We will give a short overview about this kind of interactions in the following,

evaluating the contribution to the total potential energy arising from the presence of induced dipoles in the atoms of the system's molecules coming from the fluctuations of their electron clouds. As the electronic motion is usually much faster than the intramolecular atomic motion, each molecule (say i) is considered to be formed by a set of fixed partial charges $q_{i\beta}$ associated with differences in the electronegativity of atoms leading to a deformation of molecular electron clouds. Thus, the net charge of molecule i, q_i, whose center of mass is located at $\vec{r}_i$, can be written as

$$q_i = \sum_{i\beta} q_{i\beta}, \tag{1}$$

where the index $i\beta$ runs over the atoms of the molecule i. The atomic partial charges $q_{i\beta}$ are located at the atoms' positions relative to the center of mass of the molecule, $\vec{r}^{\,0}_{i\beta}$. Allowing the fluctuations of the electronic clouds of these atoms implies that this charge is allowed to undergo oscillations over distances $\vec{d}_{i\beta}$, while the center of mass of the atom is fixed. Therefore, in this case, the total electrostatic potential created by the molecule i at a distance $\vec{R}$ from its center of mass is given by

$$V_i(\vec{R}) = \sum_{i\beta} \frac{q_{i\beta}}{4\pi\epsilon_0 |\vec{R} - \vec{r}^{\,0}_{i\beta} - \vec{d}_{i\beta}|}, \tag{2}$$

where the sum is over all atoms of the molecule i and ϵ_0 is the electric constant. A Taylor expansion of the right hand side of the previous equation around $\vec{d}_{i\beta} = 0$ straightforwardly yields[29]

$$\begin{aligned} V_i(\vec{R}) &= V_i^0(\vec{R}) \\ &\quad + \frac{1}{4\pi\epsilon_0}\left[-\sum_{\zeta} \vec{\mu}_{i\zeta} \vec{\nabla}_\zeta \frac{1}{R} + \sum_{\zeta\xi} \frac{1}{3}\theta_{i\zeta\xi} \vec{\nabla}_\zeta \vec{\nabla}_\xi \frac{1}{R} - \cdots \right] \\ &= V_i^0(\vec{R}) - \sum_{\zeta} T_\zeta \vec{\mu}_{i\zeta} + \frac{1}{3}\sum_{\zeta\xi} T_{\zeta\xi}\theta_{i\zeta\xi} - \cdots, \end{aligned} \tag{3}$$

where $\zeta, \xi = x, y, z$,

$$V_i^0(\vec{R}) = \sum_{i\beta} \frac{q_{i\beta}}{4\pi\epsilon_0 |\vec{R} - \vec{r}^{\,0}_{i\beta}|} \tag{4}$$

is the Coulomb potential due to fixed non-polarizable charges, and

$$\begin{aligned} T^{(n)}_{\zeta\xi\ldots\nu} &= \frac{1}{4\pi\epsilon_0} \vec{\nabla}_\zeta \vec{\nabla}_\xi \cdots \vec{\nabla}_\nu \frac{1}{R}, \\ \vec{\mu}_{i\zeta} &= \sum_{\beta} q_{i\beta} \vec{r}_{i\beta,\zeta}, \\ \frac{2}{3}\theta_{i\zeta\xi} &= \sum_{\beta} q_{i\beta} \vec{r}_{i\beta,\zeta} \vec{r}_{i\beta,\xi} \end{aligned} \tag{5}$$

are, respectively, the multipolar tensor, the ζ component of dipolar moment, and the (ζ, ξ) element of the quadrupolar moment of the molecule i. An extension of the expansion to higher orders is straightforward. Terms of order higher than the Coulomb potential are neglected in non-polarizable force fields. The second term on the right hand side of Eq. (3) accounts for the interactions induced by the dipoles $\vec{\mu}_{i\beta}$ and is included in the polarization methods most commonly used in MD simulations, Drude oscillators, and induced point dipoles.[25] Of course, the total field created by the molecule i in $\vec{R}$ can be directly obtained from Eq. (3), and its ζ component is given by

$$\begin{aligned} E_{i\zeta}(\vec{R}) &= E^0_{i\zeta}(\vec{R}) + \sum_{\xi} T_{\zeta\xi} \vec{\mu}_{i\xi} - \frac{1}{3}\sum_{\xi\phi} T_{\zeta\xi\phi}\theta_{i\xi\phi} - \cdots \\ &\simeq E^0_{i\zeta} + \sum_{\xi} T_{\zeta\xi}\mu_{i\xi}, \end{aligned} \tag{6}$$

where $E^0_{i\zeta}(\vec{R}) = -T_\zeta q_i$ is the field created by the fixed non-polarizable atoms.

APPLE&P uses the induced point dipole method, which relies on the expression of the dipolar moment of the atom $i\beta$,

$$\vec{\mu}_{i\beta} = \alpha_{i\beta} \cdot \vec{E}_{i\beta}, \tag{7}$$

where $\alpha_{i\beta}$ is the polarizability of the atom $i\beta$ of the molecule i and $\vec{E}_{i\beta} = \vec{E}(\vec{r}_{i\beta})$ is the total electric field acting on the atom $i\beta$. This electric field can be directly read from Eq. (6) and we get, to first order in the multipolar expansion,

$$\vec{\mu}_{i\beta} = \alpha_{i\beta}[\vec{E}^0_{i\beta} + \sum_{j=1}^{N} \sum_{j\gamma \neq i\beta} T_{i\beta j\gamma} \vec{\mu}_{j\gamma}], \tag{8}$$

which is the basic recursive equation for determining the dipoles in the system. Consequently, the inclusion of the fluctuations of the electron cloud in MD simulations leads to an additional term for the total intermolecular interaction energy, which reads

$$\begin{aligned} U_{\text{pol}} = &\underbrace{-\sum_{i=1}^{N}\sum_{i\beta} \vec{\mu}_{i\beta}\vec{E}^0_{i\beta}}_{U_{q\mu}} \underbrace{-\frac{1}{2}\sum_{i,j=1}^{N}\sum_{j\gamma\neq i\beta} \vec{\mu}_{i\beta} T_{i\beta j\gamma} \vec{\mu}_{j\gamma}}_{U_{\mu\mu}} \\ &\underbrace{+\sum_{i=1}^{N}\sum_{i\beta} \frac{\vec{\mu}^2_{i\beta}}{2\alpha_{i\beta}}}_{U_{self}}, \end{aligned} \tag{9}$$

where N is the total number of molecules in the system. $U_{q\mu}$ represents the interaction energy of the dipoles with the electrostatic field of the molecules with fixed partial charges, $U_{\mu\mu}$ stands for the dipole-dipole interaction, and U_{self} is the self-energy which is given by[30]

$$\begin{aligned} U_{self} &= \sum_{i=1}^{N}\sum_{i\beta} \int_0^{\vec{\mu}_{i\beta}} \vec{E}_{i\beta} \mathrm{d}\vec{\mu}'_{i\beta} = \sum_{i=1}^{N}\sum_{i\beta} \int_0^{\vec{\mu}_{i\beta}} \frac{\vec{\mu}'_{i\beta}}{\alpha_{i\beta}} \mathrm{d}\vec{\mu}'_{i\beta} \\ &= \sum_{i=1}^{N}\sum_{i\beta} \frac{\vec{\mu}^2_{i\beta}}{\alpha_{i\beta}}. \end{aligned} \tag{10}$$

In this study, we focus on the influence of the additional potential energy term associated with electronic polarization effects on the properties of the condensed phase of dense ionic fluids, specifically on those of mixtures of ionic liquids and lithium salts. Our main contribution over previous studies[18,31] is the evaluation of the actual influence of the electronic polarization on the behaviour of lithium salts in dense ion environments, specifically on the caging of lithium ions and, subsequently, on their transport in the bulk system, comparing the predictions of the polarizable and non-polarizable versions of specific optimized force fields.

III. SIMULATION DETAILS

In this work, we focus on the analysis on one specific mixture which consists of 250 $[EMIM]^+$, 300 $[TFSI]^-$, and 50 Li^+ (16% lithium salt). In the following, the simulation procedure for the three force fields is described. In order to achieve a description as unbiased as possible, we used the default options for both MD packages, Gromacs (OPLS-AA) and AMBER (APPLE&P) and performed NPT simulations at p = 1 atm and T = 298.15 K. Of course, due to the different parametrization of the intermolecular forces, the resulting densities of the three FFs varies: $\rho_{\text{OPLS-AA}}$ = 1.60 g cm^{-3}, $\rho_{\text{APPLE\&P-NP}}$ = 1.55 g cm^{-3}, and $\rho_{\text{APPLE\& P}}$ = 1.56 g cm^{-3}. Although being aware that even small differences in density affect the dynamic properties of the system, we believe that uniform conditions of 1 atm and 298.15 K reflect a better basis for comparison than a NVT simulation at a fixed density for all three systems as the latter method would involve simulations at different pressures for at least two simulation systems.

A. Simulations with non-polarizable force field (OPLS-AA)

The non-polarizable simulations of mixtures reported in this paper were performed by means of the Gromacs 4.6.7 package.[32] The FF chosen for carrying out the parametrization of all species present in the system was OPLS-AA (developed by Jorgensen[27] for organic liquids), in which every atom appears explicitly. The imidazolium cation was modeled using the all-atom representation of the CH_2 and CH_3 groups in the alkyl chain, and also of the methyl group bonded to the imidazolium ring. Lithium cations were modeled by a single site of charge +1. $[TFSI]^-$ was modeled as a set of 15 sites whose partial charges were reported in a previous article by Canongia-Lopes and Pádua.[33] Méndez-Morales *et al.*[10] have shown that these parameters give predictions for the local environment of lithium ions which are close to the experimental results.

Long-range electrostatic interactions were treated by using the Particle-Mesh Ewald (PME)[34] method with a grid spacing of 12 nm and cubic interpolation. A cutoff distance of 1.1 nm was used for Lennard-Jones interactions, and a neighbor searching was made up to this same distance from the central ion and was updated every five simulation steps. The Linear Constraint Solver (LINCS) algorithm[35,36] with a fourth-order expansion of the constraint coupling matrix was used to hold the bonds rigid, and long range dispersion corrections were used for both energy and pressure.

A conjugated gradients algorithm was used to minimize the energy of the system, removing all bad contacts resulting from the initial random configuration of ions. The maximum step size and the tolerance were set to 0.01 nm and 0.1 kJ nm^{-1} mol^{-1}, respectively.

Finally, the system passed through two NPT simulations: a 20 ns stabilization was followed by a 10 ns simulation run. The time step of the simulations was 2 fs. For these steps, and to control the temperature and pressure of the system, a V-rescale thermostat[37] with a temperature coupling constant of 0.1 ps and a Parrinello-Rahman barostat[38] were used, respectively. The barostat had a reference pressure of 1 bar, an isothermal compressibility of 4.5×10^{-5} bar^{-1}, and a relaxation time of 0.1 ps. NVT simulations were also performed, but no relevant differences were detected for the studied systems.

B. Simulations with polarizable force fields (APPLE&P)

The simulation was performed with the MD-simulation package AMBER 10.[39] This software was extended in order to include a Buckingham potential and a Thole screening[11] which was necessary to use the many body polarizable force field APPLE&P.[21]

The starting structure was produced randomly in the gas phase in a cubic box with a length of 300 Å. First, the simulation cell was shrunk. Second, an equilibration run of 10 ns in the NPT ensemble at 1 bar with polarization was performed to obtain a homogeneous system. The averaged density was used for the followed production run in the NVT ensemble. The Berendsen thermostat was used to control the temperature and the Shake algorithm to constraint the bonds containing hydrogen. The elementary integration step was 1 fs. The electrostatic interactions were calculated via the PME method (Ewald coefficient, 0.275 11; grid size, 48 × 45 × 45; interpolation order, 4). The simulation time employed in the production runs with the APPLE&P force field was 20 ns.

We used the same simulation setup but switching off the polarization (non-polarizable APPLE&P, hereafter denoted as APPLE&P-NP) to estimate the order of magnitude of the influence of the polarization on systems containing lithium salts.

IV. RESULTS AND DISCUSSION

A. Structural properties

The testing of the accuracy of the OPLS-AA non-polarizable potential for the calculation of structural properties of mixtures of imidazolium-based ILs and Li salts with a common anion has been previously reported by Méndez-Morales *et al.*,[10] who compared the calculated densities of ILs of the imidazolium families to their experimental values, and hence we shall not give any further details here. In order to test the structural predictions of the APPLE&P force fields, we calculated, for all of them, radial distribution functions (RDFs),

$$g_{ij}(r_{12}) = \frac{1}{\rho_i \rho_j} \sum_{i,j} \langle \delta(\vec{r}_1 - \vec{r}_i)\delta(\vec{r}_2 - \vec{r}_j)\rangle \tag{11}$$

for different species around lithium ions, where ρ_k is the number density of species k, the sum extends over all ions of species i and j, and brackets indicate the equilibrium ensemble average. Moreover, we also calculated the number of ions around a central ion as a function of distance according to

$$n(r) = 4\pi\rho_\infty \int_0^r dr\, r'^2 g(r'), \tag{12}$$

where ρ_∞ is the bulk number density of the specific species, and plot them as a function of the distance, which provides insights into the accumulation of ions/molecules around lithium ions. Eq. (12) assumes spherical molecules as a central ion. The OPLS-AA, APPLE&P-NP, and APPLE&P predictions for these magnitudes are presented in Fig. 2. In this figure, we can see that APPLE&P, APPLE&P-NP, and OPLS-AA lead to broadly similar structural predictions, but some important differences between the force fields can be also observed. First, we can see that APPLE&P gives a narrower and higher peak in the Li-$O_{[TFSI]^-}$ than the other two potentials. The effect is the opposite in the case of Li^+-$N_{[TFSI]^-}$ and Li^+–$[EMIM]^+$ RDFs. In the first case, the first peak of the RDF is shifted towards larger distances by using the polarizable APPLE&P, while in the second case it is visible that the equilibrium distance decreases. This suggests that the electronic polarization weakens the interionic coupling, very much like an enhanced screening of the Coulomb potential would do. Schmollngruber *et al.* reported similar results by systematically studying the influence of polarization for pure ionic liquids.[25] This same behavior was reported by Bedrov *et al.*,[18] who calculated cation/cation, cation/anion, and anion/anion center-of-mass RDFs for various ILs at 393 K and atmospheric pressure. Their calculated peaks in $g(r)$ by switching off the polarization of APPLE&P were narrower and higher as compared to those of the polarizable APPLE&P. They also concluded that the effect of polarization is to weaken the structuring of the liquid or the spatial interionic correlations. However, this enhanced structuring of the IL in the case of the polarizable FF is somehow unexpected, as Bedrov *et al.*[18] also concluded, since the energy per ion pair in the liquid phase predicted by the non-polarizable model is actually lower than the one obtained using the polarizable FF, and they also stated that no enhancement of structuring upon turning off the polarization was detected in various nonionic liquids. The small effect observed in the Li–O and Li–N RDFs, when comparing APPLE&P and OPLS-AA, is similar to that found in the work by Yan *et al.*[19] Interestingly, switching off the polarization leads to only one single peak in the Li–N RDF and, thus, the coordination behavior of TFSI on lithium ions is strongly affected, which is in good agreement with previous results by Lesch *et al.*,[13] who studied the influence of decreasing the polarizability of TFSI oxygens.

More specifically, the Li^+-$[EMIM]^+$ RDF with respect to the center of mass is plotted in Fig. 2, where it can be seen that APPLE&P and OPLS-AA lead to essentially similar behavior, but with important differences mainly in the structure of the first peak. The peaks of the RDFs of the APPLE&P potentials are located at slightly shorter distances due to the weakened Coulomb repulsion predicted by the polarizable force field. Moreover, we can see in $g_{Li^+ - [EMIM]^+}$ that the double first peak predicted by the APPLE&P based force fields virtually disappears using OPLS-AA. Neglecting the polarization in APPLE&P leads to small changes in the Li^+-IL cation RDF in terms of distances and intensities but the agreement with original APPLE&P is still better than using OPLS-AA. However, the relative populations of the two coordination modes predicted by the APPLE&P based force fields are more similar in the case of the polarizable potential than for APPLE&P-NP, which shows a much higher peak at 0.75 nm than at 0.5 nm. Figure 2 also shows that IL cations only appear from the second coordination shell of the Li^+ ions onwards,

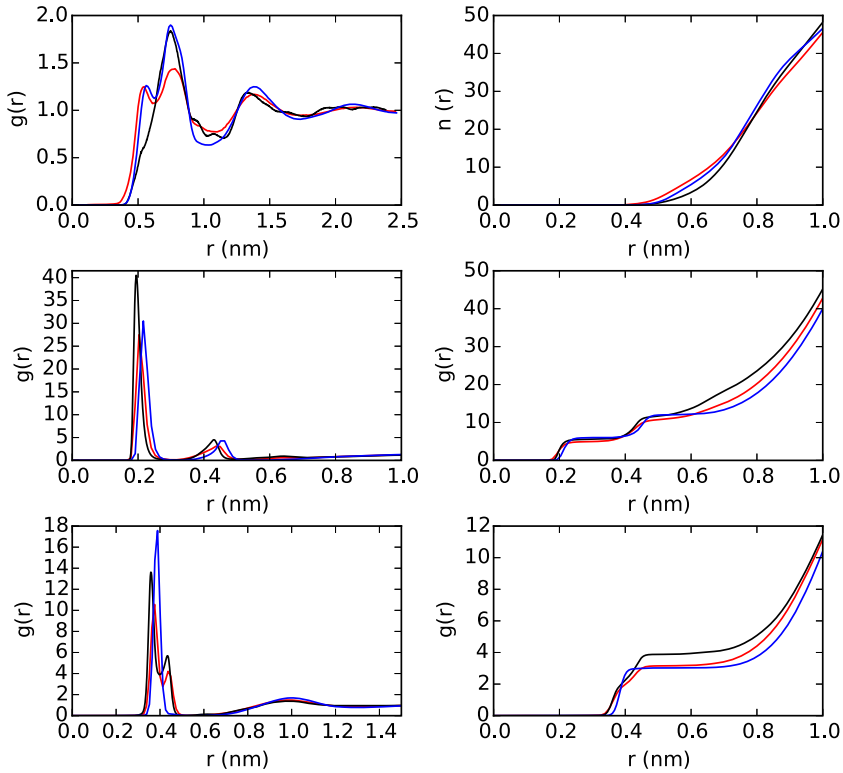

FIG. 2. Comparison of (top) Li^+–$[EMIM]^+$, (middle) Li^+–O of $[TFSI]^-$, and (bottom) Li^+–N of $[TFSI]^-$ RDFs and corresponding coordination numbers for the different potentials: APPLE&P (red), APPLE&P-NP (blue), OPLS-AA (black).

as expected, emphasizing that the first coordination shell of lithium ions is formed by $[TFSI]^-$ anions. Besides, the coordination numbers are considerably higher for the polarizable APPLE&P and its nonpolarizable homologue in the region between 0.4 and 0.8 nm. After that, OPLS-AA predictions exceed those of the APPLE&P and are approximately equal to those of APPLE&P-NP.

On the other hand, in the same figure, we can observe that Li^+ ions are strongly coordinated with the oxygen atoms of the $[TFSI]^-$ anions, as indicated by the heights of their first and overwhelmingly dominating peaks. The double peak structure in the Li^+–N RDF is associated with monodentate (C_{4v}) and bidentate (C_{2v}) coordination modes, whose meaning has been extensively analyzed in previous studies.[10,13,40–42] Both first peaks are slightly shifted to larger distances with the polarizable FF, while the rest of the RDFs are essentially unaffected and for $r \geq 8$ Å similar RDFs for both FFs can be observed. Once again, this indicates that the onset of the electronic density fluctuation associated with the polarizable potential simulations weakens the Li–O and Li–N coordination and, therefore, the average interionic distance decreases accordingly.[25] Interestingly, the double peak structure in the Li^+–N RDF vanishes by switching off the polarization in APPLE&P and the bidentate coordination mode of $[TFSI]^-$ on lithium ions is largely preferred, as intensively discussed in a previous study.[13]

The coordination numbers in Fig. 2 (right column) indicate that the structural predictions of OPLS-AA and the two APPLE&P based force fields are quite similar, but, once again, notable differences are also registered. Both FFs predict a similar local environment of lithium ions as reflected by the plateaus in the Li^+–O_{TFSI} and Li^+–N_{TFSI} $n(r)$, that can be interpreted as two closed and compact coordination shells.[43] Moreover, the number of IL cations coordinating lithium ions is slightly increased by electronic fluctuations at the shorter distances (0.4 nm to 0.8 nm) and a crossover is registered at larger distances, while the electronic polarization decreases the number of $[TFSI]^-$ anions in the first coordination shells of Li^+ (up to 1 nm). The first coordination shell of Li^+ ions is made up essentially of IL anions, with lithium ions being strongly bound to O_{TFSI}, which form the inner part of their first solvation shell (plateau extending from 0.19 nm to 0.4 nm). The outer part of the first coordination shell (up to 0.8 nm) is made up of both oxygen atoms and nitrogen atoms of $[TFSI]^-$ anions, and extends from 0.4 nm to 0.8 nm both for the polarizable and nonpolarizable FFs. However, it is in this latter case where the most notable difference between the force fields is registered in what structure is concerned. The number of O_{TFSI} and N_{TFSI} atoms predicted by the polarizable FF in this part of the shell is consistently smaller than that of their non-polarizable counterpart: the coordination numbers predicted by the three force fields differ notably between 0.5 and 0.75 nm, where OPLS-AA predicts a coordination number of 4 while the APPLE&P based ones predict only 3. Finally, the small shoulder at $r \approx 0.37$ nm indicates the bidentate coordination of $[TFSI]^-$ and it is visible with and without electronic density fluctuations in the FF. In contrast, using APPLE&P-NP leads to a slightly different local environment of lithium ions since the plateaus are more pronounced and only one coordination state for TFSI is observed. This is in good agreement with previous studies of the influence of TFSI oxygen polarizability on simulation results.[13]

To sum up, the structural picture of the three potentials is essentially similar, but OPLS-AA visibly tends to favor the presence of anions close to Li^+ cations compared to APPLE&P-based potentials, while reducing that of the IL cations, in agreement with the stronger Coulomb coupling shown by the former nonpolarizable potential. The overall picture emerging from these RDFs and coordination numbers is that the electronic polarization reduces the correlation strength of Li^+ with its first solvation shell, which should lead to an easier diffusion of the added salt cations in the bulk mixtures, with the subsequent enhancement of the transport coefficients of these systems. Contrary to what happens in the gas phase, the increased presence of a background of dipolar moments in condensed phases (macroscopically described by an enhanced dielectric constant), either coming from the onset of electronic fluctuations in the molecules or from the addition of molecular cosolvents, reduces the strengths of the Coulomb interactions. As in ionic liquids most parts of the cohesion of the dense ionic condensed phase comes from the Coulomb interionic interactions, which inevitably leads to a weakening of the interionic global interaction. Indeed, this could be also interpreted as the polarizability associated with electronic fluctuations acting as an inner solvent that screens electrostatic interionic interactions, as pointed out by some of us in a recent paper.[25]

In order to gain further insight into the molecular environment of the ions in the mixture and its influence on their single-particle dynamics, we calculated the cage correlation functions (CaCFs)[44] of Li^+,

$$\mathrm{CaCF}(t) = \frac{\langle B(t)B(0)\rangle}{\langle B^2(0)\rangle}, \tag{13}$$

where $B(t)$ takes the value of 1 if O_{TFSI} is inside the first coordination shell of Li^+ and is zero otherwise. The brackets indicate the average over all time origins. The predictions of the three potentials are shown in Fig. 3, where it can be seen that the cage is much more resilient in the case of nonpolarizable potentials. Indeed, after 10 ns CaCF(t) still retains 99.8% of its initial value using OPLS-AA, while for the polarizable potential it is a mere 97% after 1 ns and 85% at the end of the simulated range. Switching off the polarization of APPLE&P leads to a more stable cage but the decrease is slightly faster than using OPLS-AA parameters. The results reinforce the interpretation that the electronic polarization weakens the correlations inside the bulk media, leading to more mobile ionic species. Similar trends/results were also obtained by studying different polarizability states of TFSI oxygens.[13]

To sum up, the effect of polarization coming from electronic fluctuations on the structure of the analyzed IL-lithium salt mixture seems to be perturbatively small, and non-polarizable potentials apparently provide a good enough description of the main structural features of this dense ionic mixture. However, as it is well known,[15,16] taking the electron cloud into account has a strong impact on transport properties such as diffusion coefficients. Single-particle dynamics of the mixtures is analyzed in the following.

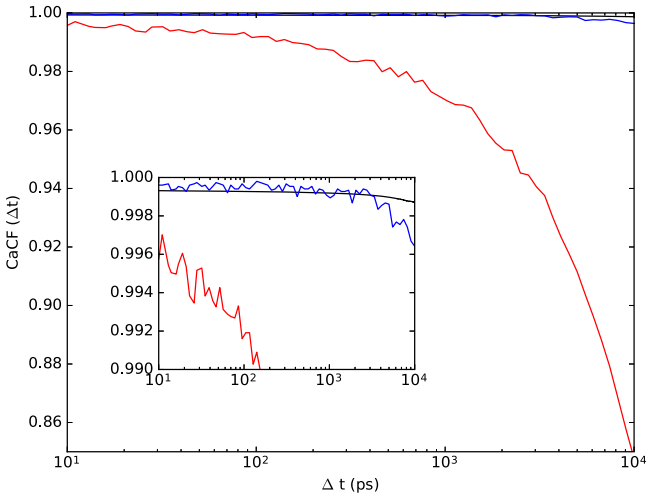

FIG. 3. Cage correlation function of Li^+ for a Li[TFSI]-[EMIM][TFSI] (1:5) mixture calculated with APPLE&P (red line), APPLE&P-NP (blue line), and OPLS-AA (black line).

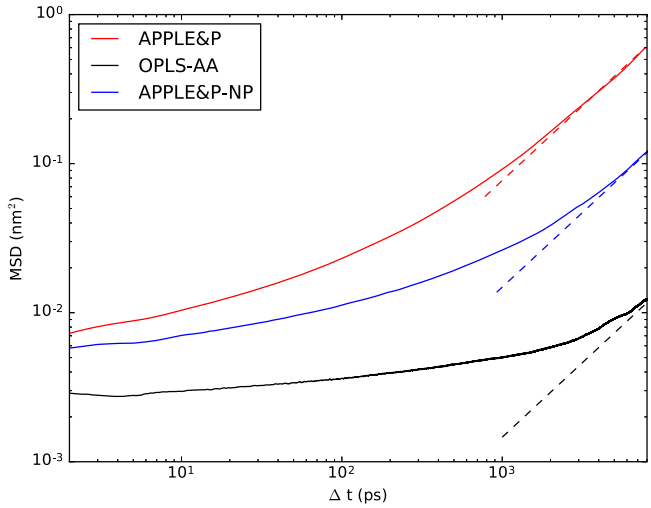

FIG. 4. Comparison of the influence of polarization on the MSD of lithium. The dashed lines represent unit slope lines.

B. Dynamical properties

In order to shed more light on the effect of electronic polarization in the dynamical properties, we calculated the mean-squared displacements (MSDs) for determining the transport properties as well as velocity autocorrelation functions (VACFs) and their Laplace transforms to characterize the type of motion.

The first magnitude is defined as

$$\langle(\Delta\vec{r}_i)^2\rangle = \langle(\vec{r}_i(t) - \vec{r}_i(0))^2\rangle, \tag{14}$$

where $\langle\ldots\rangle$ denotes averaging over all the atoms in the simulation box. It is expected that the MSDs behave like $\langle(\Delta\vec{r}_i)^2\rangle \propto t^2$ at short times (ballistic regime) and grow linearly in the limit $t \to \infty$ (Brownian motion) if the system is liquid. Intermediate subdiffusive plateaus are indicative of long caging times for the diffusive species at intermediate times, being this subdiffusive dynamics (for which $\langle(\Delta\vec{r}_i)^2\rangle \propto t^\beta$ with $\beta < 1$) characteristic of glass formers.[45,46] Moreover, MSDs are related to the diffusion coefficients of the species present in the mixture through the well-known relation[47]

$$D_i = \lim_{\Delta t\to\infty} \frac{\langle(\vec{r}_i(t+\Delta t) - \vec{r}_i(t))^2\rangle}{6\Delta t}. \tag{15}$$

In order to study the influence of the electronic polarization on the lithium ion transport, we focus on the mean-squared displacement of lithium ions. The corresponding results are presented in Fig. 4, where we can see that in all the studied cases the diffusive regime has been reached, as shown by the unit slope line in the log-log plot. There it can also be seen that taking the electron cloud into account leads to larger values for the MSD. This is once again related to the fact that the polarization acts as an inner screening solvent which weakens the Coulomb interaction.[25] Interestingly, OPLS-AA and APPLE&P-NP differ in one order of magnitude. Thus, introducing the polarizability into OPLS-AA is not sufficient to achieve results for dynamical properties comparable to experiments, and its parameters would have to be adjusted in addition to add polarizabilities. However, the comparison of APPLE&P with APPLE&P-NP indicates that neglecting the fluctuations of the electron clouds leads to a significantly smaller MSD, in good agreement with previous studies.[18,25]

Finally, we further clarify the single-particle dynamics of the Li^+ ions in the mixture determining the normalized VACFs,

$$C(t) = \frac{\langle\vec{v}(t)\cdot\vec{v}(0)\rangle}{\langle\vec{v}(0)\cdot\vec{v}(0)\rangle}, \tag{16}$$

where $\vec{v}(t)$ is the velocity of the center of mass of the molecule at time t and $\langle\ldots\rangle$ indicates the ensemble average. These correlation functions can be seen in Fig. 5 for the different components of the mixture. In the case of lithium ions, they show a damped periodic oscillation after the first collision associated with a rattling motion of the ions inside their cages. The correlation functions of the other ionic species do not show oscillations, and a monotonic transition to the diffusive regime is observed. According to Kato *et al.*,[48] the initial decay of $C(t)$ can be used to estimate the mean squared forces

$$C(t) = 1 - \frac{\langle F^2\rangle}{3mk_BT}\frac{t^2}{2!} + \mathcal{O}(t^4) \tag{17}$$

acting on the respective ions with a mass m. Using the first 50 fs for the fitting, the mean-squared forces $\langle F^2\rangle$ in Table I are obtained. The forces on lithium are the strongest, which can easily be explained by the strong cage around these ions. Since the anions are most involved in this cage, forces on them are weaker compared to lithium but stronger than those acting on the imidazolium ions.

Interestingly, the forces on imidazolium and the TFSI anion are very similar in the APPLE&P force fields and seem not to depend on the polarizable forces. In contrast, the different mean-squared forces on lithium are significant and may explain the drastic change in the cage correlation function in Fig. 3.

Table I shows the diffusion coefficients for all three potentials. It is clearly indicated that the non-polarizable OPLS-AA leads to the smallest diffusion coefficients. This is consistent with Fig. 4. The difference to non-polarizable APPLE&P is roughly one order of magnitude for all three species, which can be related to stronger Coulombic coupling associated with the lack of electronic polarization. The

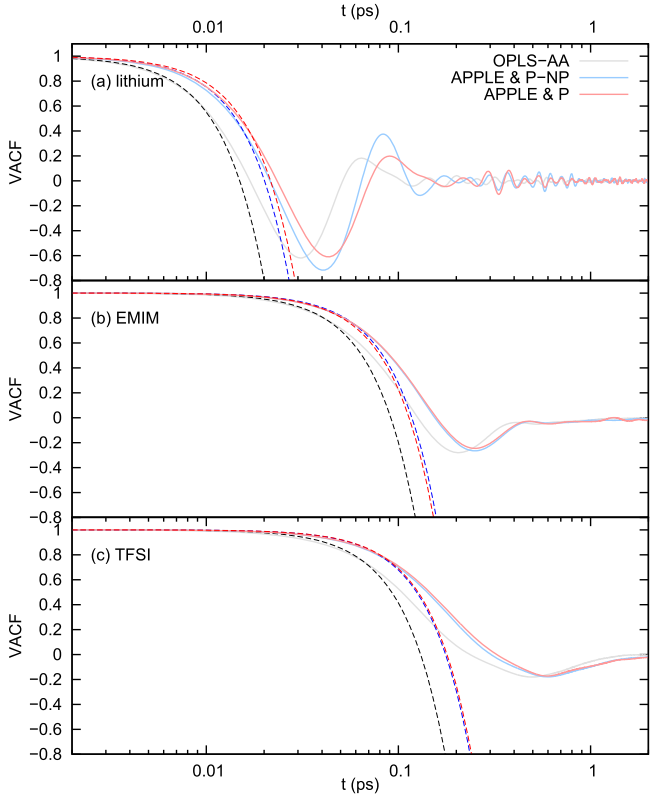

FIG. 5. Comparison of the velocity autocorrelation functions in the [EMIM][TFSI] mixture: (a) Li^+, (b) $[EMIM]^+$, and (c) $[TFSI]^-$. The dashed lines represent the fit according to Eq. (17).

step from non-polarizable to polarizable APPLE&P is another order of magnitude. Thus, OPLS-AA and APPLE&P differ by almost two orders of magnitude, so we can easily conclude that a direct addition of polarization to OPLS-AA is not sufficient to bridge the gap with the polarizable force field, which in previous studies[11,18] was clearly seen to show an excellent agreement with experimental results.

On the other hand, the frequencies of cage relaxations can be obtained from the Laplace transform of the VACF,[47] which is often referred to as the power spectrum as it should reflect via the Wiener-Khinchin theorem the squared Fourier transform of the velocities.[47,49] Since we are interested in the mutual motion of the ions and not in their intramolecular vibrations, the velocity auto-correlation function is not calculated for each atom separately (as performed in Ref. 49) but for the center-of-mass velocity. Consequently, quantum-mechanical corrections as mentioned in Ref. 50 are not necessary for our discussion.

The Laplace spectra in Fig. 6 show again the fundamental difference between the OPLS-AA on the one side and the (non-)polarizable APPLE&P on the other. Interestingly, both APPLE&P force fields result in similar power spectra for EMIM and TFSI, indicating that the induced forces are not so important for their mutual motion. This situation is different for lithium. Here, a shift to lower frequencies is observed for the polarizable force field. Obviously, lithium is much more sensitive to polarizability than the other ions. Finally, it is noteworthy that, in all cases but in a specially remarkable way for lithium cations, the spectra are red-shifted by the addition of electronic fluctuations confirming once again that the effect of the polarizability of the electron clouds is to soften Coulomb interactions in the bulk, hence leading to faster diffusions of the ionic species.

Furthermore, the spectra are crowded below 100 cm^{-1} for EMIM and TFSI indicating a more translational than librational motion for these ions. For the OPLS-AA force field, the long-frequency tail is a little bit more pronounced. In contrast, the peaks in the power spectrum of Li^+ at these frequencies are rather low for all applied FFs. The major contributions can be found between 200 and 500 cm^{-1} for the (non-)polarizable

TABLE I. Dynamic properties of the ions as a function of the force field.

	D ($Å^2$/ps)	$\langle F^2 \rangle$ (nN^2)
	OPLS-AA	
EMIM	$5.6 \cdot 10^{-5}$	0.55
TFSI	$3.9 \cdot 10^{-5}$	0.67
Li	$1.7 \cdot 10^{-5}$	1.28
	APPLE&P-NP	
EMIM	$1.1 \cdot 10^{-3}$	0.33
TFSI	$4.2 \cdot 10^{-4}$	0.37
Li	$2.5 \cdot 10^{-4}$	0.70
	APPLE&P	
EMIM	$3.8 \cdot 10^{-3}$	0.35
TFSI	$1.6 \cdot 10^{-3}$	0.36
Li	$9 \cdot 10^{-4}$	0.61

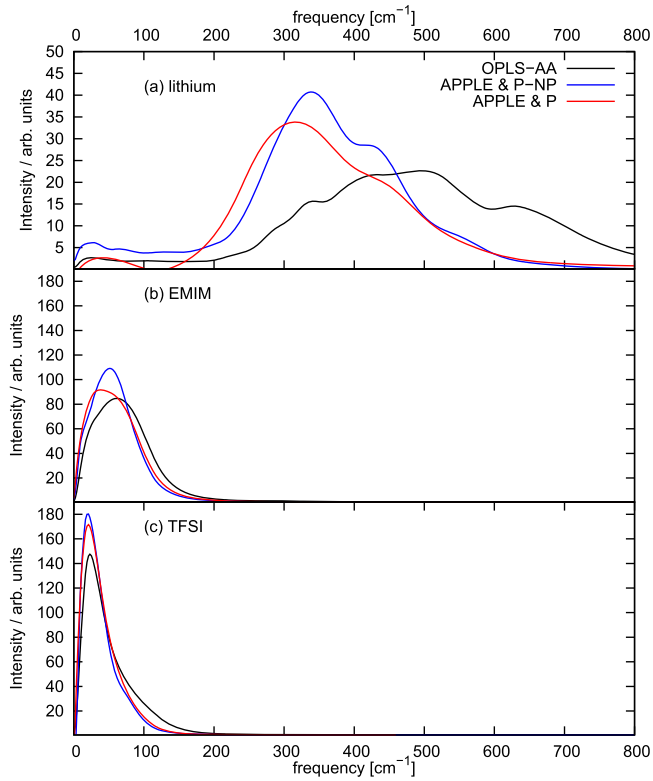

FIG. 6. Laplace transform of the velocity auto-correlation function of the ions obtained from the three FFs smoothed by a Bezier function.

APPLE&P and 300-750 cm^{-1} for OPLS-AA. Here, the librational motion within cages dominate as already expected by the sub-diffusive regions in Fig. 4.

Finally, we must also mention that some differences in the studied transport properties could be due to variations in the density predicted by the different force fields. As it is well known, MD of dense liquid systems can be considerably affected by even small changes in density,[51] and this correlation has been recently studied by Sun *et al.* for ionic liquids.[52] Due to close packing in these systems, the forces between them in conventional liquids arise almost exclusively from the harsh short-ranged repulsive interactions between nearest neighbors, so volume effects are expected to significantly affect molecular motions in liquids. This is, of course, also the case of ionic liquids, where Coulomb interactions also come into play. In our case, the small but significant differences in the density predicted by the studied potentials are expected to have a real influence on the behaviour of the transport properties. Particularly, one can see that the density predicted by OPLS-AA is considerably larger than the others. This is in agreement with the stronger coupling associated with the situation where the electronic fluctuations are not present and can help us understand the larger Li–N and Li–O coordination numbers predicted by this potential. In the case of the polarizable APPLE&P and the nonpolarizable APPLE&P-NP we see the same effect, but in this case the nonpolarizable version leads to smaller densities, probably due to the latter potential not being optimized for nonpolarizable situations. In what transport coefficients are concerned, density effects can also be observed in the studied magnitudes, but their actual extent is problematic since it is difficult to separate from other contributions (temperature and force field parametrizations, among others) in the absence of more systematic simulations at different pressures.

V. CONCLUSIONS

We have studied the effect of the electronic polarization via simulations of [EMIM][TFSI] doped with a lithium salt with a common anion using the well-known nonpolarizable force field OPLS-AA and the polarizable force field APPLE&P. In our study, we mainly focused on the influence of polarization and the question if adding polarization to OPLS-AA is sufficient to overcome the gap between OPLS-AA and APPLE&P.

In order to quantify the actual influence of the electronic polarization on systems containing lithium salts, we have switched off the polarization in APPLE&P, while OPLS-AA has been used as a structural reference for the other force fields due to its well-known accuracy in describing the structure of these mixtures. We have seen that the main effect of electronic fluctuations is a perturbative weakening of the Coulomb interactions in the bulk system. This leads to structural modifications as reflected by the radial distribution functions and coordination numbers, where the distances between the various species in the mixture show these decreased interactions. The RDFs clearly indicate that adding the polarization leads to strong structural changes. Thus, a simple direct addition of the electronic polarization to OPLS-AA can lead to a marked disagreement with experimental results. Moreover, we have seen that polarizable potentials notably reduce the cage confinement of the Li^+ cations, leading to a much earlier onset of the diffusive regime and a virtual suppression of the intermediate subdiffusive plateaus predicted by non-polarizable force fields. Furthermore, simply polarizing OPLS-AA does not bridge the gap between OPLS-AA and APPLE&P and induces structural changes in disagreement with experiments. Finally, we calculated velocity autocorrelation functions and their Fourier transforms, the vibrational densities of states of the species in the mixture, and we showed that the main effect of electronic polarization is a red-shifting of the normal modes comparing OPLS-AA and polarizable APPLE&P for our system. The theoretical description of this transformation of the vibrational spectrum is now in progress.

ACKNOWLEDGMENTS

The financial support of the Spanish Ministry of Economy and Competitiveness (Project Nos. MAT2014-57943-C3-1-P and FIS2012-33126) is gratefully acknowledged. Moreover, this work was funded by the Xunta de Galicia through the Galician Network on Ionic Liquids (REGALIS, CN 2014/015) and the Agrupación Estratéxica de Física (Grant No. AGRUP2015/11). All these research projects were partially supported by FEDER. T. M.-M. thanks the Spanish Ministry of Education for her FPU grant. Facilities provided by the Galician Supercomputing Centre (CESGA) are also acknowledged. V. L. and A. H. acknowledge the BMBF within the SafeBatt project (Foerderkennzeichen: 03X4631N) for financial support. The authors would also like to acknowledge the scientific network supported by the COST Action No. CM1206. Finally, we thank Diddo Diddens, Jens Smiatek, and Dmitry Bedrov for scientific discussion and Markus Blank-Burian for the technical support in Münster.

[1] R. D. Rogers and K. R. Seddon, Science **302**, 792 (2003).
[2] P. Wasserscheid and T. Welton, *Ionic Liquids in Synthesis* (Wiley Online Library, 2003).
[3] J. Dupont, R. F. de Souza, and P. A. Z. Suarez, Chem. Rev. **102**, 3667 (2002).
[4] M. V. Fedorov and A. A. Kornyshev, Chem. Rev. **114**, 2978 (2014).
[5] S. Seki, Y. Kobayashi, H. Miyashiro, Y. Ohno, A. Usami, Y. Mita, N. Kihira, M. Watanabe, and N. Terada, J. Phys. Chem. B **110**, 10228 (2006).
[6] G. B. Appetecchi, M. Montanino, A. Balducci, S. F. Lux, M. Winterb, and S. Passerini, J. Power Sources **192**, 599 (2009).
[7] J. Lassègues, J. Grondin, C. Aupetit, and P. Johansson, J. Phys. Chem. A **113**, 305 (2009).
[8] F. Castiglione, E. Ragg, A. Mele, G. B. Appetecchi, M. Montanino, and S. Passerini, J. Phys. Chem. Lett. **2**, 153 (2011).
[9] Z. Li, G. D. Smith, and D. Bedrov, J. Phys. Chem. B **116**, 12801 (2012).
[10] T. Méndez-Morales, J. Carrete, S. Bouzón-Capelo, M. Pérez-Rodríguez, O. Cabeza, L. J. Gallego, and L. M. Varela, J. Phys. Chem. B **117**, 3207 (2013).
[11] V. Lesch, S. Jeremias, A. Moretti, S. Passerini, A. Heuer, and O. Borodin, J. Phys. Chem. B **118**, 7367 (2014).
[12] Z. Li, O. Borodin, G. D. Smith, and D. Bedrov, J. Phys. Chem. B **119**, 3085 (2015).
[13] V. Lesch, Z. Li, D. Bedrov, O. Borodin, and A. Heuer, Phys. Chem. Chem. Phys. **18**, 382 (2016).
[14] O. Borodin, Mater. Res. Soc. Proc. **1082**, Q06 (2008).
[15] J. N. C. Lopes and A. A. Pádua, Theor. Chem. Acc. **131**, 1 (2012).
[16] F. Dommert, K. Wendler, R. Berger, L. Delle Site, and C. Holm, ChemPhysChem **13**, 1625 (2012).
[17] O. Russina, R. Caminiti, T. Méndez-Morales, J. Carrete, O. Cabeza, L. Gallego, L. Varela, and A. Triolo, J. Mol. Liq. **205**, 16 (2015).

[18]D. Bedrov, O. Borodin, Z. Li, and G. D. Smith, J. Phys. Chem. B **114**, 4984 (2010).
[19]T. Yan, C. J. Burnham, M. G. D. Pópolo, and G. A. Voth, J. Phys. Chem. B **108**, 11877 (2004).
[20]O. Borodin, G. D. Smith, and W. Henderson, J. Phys. Chem. B **110**, 16879 (2006).
[21]O. Borodin, J. Phys. Chem. B **113**, 11463 (2009).
[22]G. D. Smith, O. Borodin, S. P. Russo, R. J. Rees, and A. F. Hollenkamp, Phys. Chem. Chem. Phys. **11**, 9884 (2009).
[23]C. J. F. Solano, S. Jeremias, E. Paillard, D. Beljonne, and R. Lazzaroni, J. Chem. Phys. **139**, 034502 (2013).
[24]C. Schröder, T. Sonnleitner, R. Buchner, and O. Steinhauser, Phys. Chem. Chem. Phys. **13**, 12240 (2011).
[25]M. Schmollngruber, V. Lesch, C. Schröder, A. Heuer, and O. Steinhauser, Phys. Chem. Chem. Phys. **17**, 14297 (2015).
[26]C. Schröder, Phys. Chem. Chem. Phys. **14**, 3089 (2012).
[27]W. L. Jorgensen, J. Phys. Chem. **90**, 1276 (1986).
[28]T. Mendez-Morales, J. Carrete, J. R. Rodriguez, O. Cabeza, L. J. Gallego, O. Russina, and L. M. Varela, Phys. Chem. Chem. Phys. **17**, 5298 (2015).
[29]A. Stone, *The Theory of Intermolecular Forces* (Oxford University Press, 2013).
[30]H. Yu and W. F. van Gunsteren, Comput. Phys. Commun. **172**, 69 (2005).
[31]C. Schröder and O. Steinhauser, J. Chem. Phys. **133**, 154511 (2010).
[32]D. V. D. Spoel, E. Lindahl, B. Hess, A. R. V. Buuren, E. Apol, P. J. Meulenhoff, D. P. Tieleman, A. L. T. M. Sijbers, K. A. Feenstra, R. V. Drunen, and H. J. C. Berendsen, Gromacs User Manual Version 4.6.7, 2014, http://www.Gromacs.org.
[33]J. N. Canongia-Lopes and A. A. H. Pádua, J. Phys. Chem. B **108**, 16893 (2004).
[34]T. Darden, D. York, and L. Pedersen, J. Chem. Phys. **98**, 10089 (1993).
[35]B. Hess, H. Bekker, H. J. C. Berendsen, and J. G. E. M. Fraaije, J. Comput. Chem. **18**, 1463 (1997).
[36]B. Hess, J. Chem. Theory Comput. **4**, 116 (2007).
[37]G. Bussi, D. Donadio, and M. Parrinello, J. Chem. Phys. **126**, 014101 (2007).
[38]M. Parrinello and A. Rahman, J. Appl. Phys. **52**, 7182 (1981).
[39]D. A. Case, T. A. Darden, T. E. I. Cheatham, C. L. Simmerling, J. Wang, R. E. Duke, R. Luo, M. Crowley, R. C. Walker, W. Zhang *et al.*, AMBER 10, University of California, San Francisco (2008), available at https://infoscience.epfl.ch/record/121435/files/Amber10i.pdf.
[40]S. Niu, Z. Cao, S. Li, and T. Yan, J. Phys. Chem. B **114**, 877 (2010).
[41]D. M. Seo, O. Borodin, S.-D. Han, P. D. Boyle, and W. A. Henderson, J. Electrochem. Soc. **159**, A1489 (2012).
[42]J. Pitawala, A. Martinelli, P. Johansson, P. Jacobsson, and A. Matic, J. Non-Cryst. Solids **407**, 318 (2015).
[43]V. Lesch, A. Heuer, C. Holm, and J. Smiatek, Phys. Chem. Chem. Phys. **17**, 8480 (2015).
[44]C. Schröder, J. Chem. Phys. **135**, 024502 (2011).
[45]M. G. D. Pópolo and G. A. Voth, J. Phys. Chem. B **108**, 1744 (2004).
[46]T. Méndez-Morales, J. Carrete, O. Cabeza, L. J. Gallego, and L. M. Varela, J. Phys. Chem. B **115**, 6995 (2011).
[47]D. Frenkel and B. Smit, *Understanding Molecular Simulation: From Algorithms to Applications* (Academic Press, 2001), Vol. 1.
[48]T. Kato, K. Machida, M. Oobatake, and S. Hayashi, J. Chem. Phys. **89**, 3211 (1988).
[49]K. Wendler, M. Brehm, F. Malberg, B. Kirchner, and L. delle Sitte, J. Chem. Theory Comput. **8**, 1570 (2012).
[50]R. Ramírez, T. López-Ciudad, P. Padma Kumar, and D. Marx, J. Chem. Phys. **121**, 3973 (2004).
[51]H. Parkhurst, Jr. and J. Jonas, J. Chem. Phys. **63**, 2698 (1975).
[52]L. Sun, O. Morales-Collazo, H. Xia, and J. F. Brennecke, J. Phys. Chem. B **119**, 15030 (2015).